SCALING OF GAS TURBINE FROM AIR TO REFRIGERANTS FOR ORGANIC RANKINE CYCLE (ORC) USIING SIMILARITY CONCEPT

Choon Seng Wong[1]*, Prof. Susan Krumdieck[2]

[1,2]Department of Mechanical Engineering, University of Canterbury,
Private Bag 4800, Christchurch 8041, New Zealand.
choon.wong@pg.canterbury.ac.nz[1], susan.krumdieck@canterbury.ac.nz[2]

* Corresponding Author

ABSTRACT

Organic Rankine Cycle (ORC) could be used to generate power from low temperature heat sources or improve overall cycle efficiency in waste heat applications with minimal environmental pollution. The design and development of an ORC turbine, however, is a complex and costly engineering problem. The common refrigerants for an ORC application exhibit non-ideal gas behaviour and some unfavourable characteristics, such as flammability and toxicity. These characteristics further increase the complexity of the design and laboratory testing process of a turbine. Similitude, or similarity concept, is an essential concept in turbomachinery to allow the designer to scale a turbine design to different sizes or different working fluids without repeating the whole design and development process. Similarity concept allows the testing of a turbo-machine in a simple air test bench instead of a full scale ORC test bench. The concept can be further applied to adapt an existing gas turbine as an ORC turbine using different working fluids.

This paper aims to scale an industrial gas turbine to different working fluids, other than the fluid the turbine was originally designed for. Three different approaches using the similarity concept were applied on the turbine performance data using compressed air to generate the performance curve for two refrigerants, namely R134a and R245fa. The scaled performance curves derived from the air performance data were compared to the performance map generated using 3D computational fluid dynamics (CFD) analysis tools for R134a and R245fa. The three approaches were compared in term of the accuracy of the performance estimation, and the most feasible approach was selected. The result shows that complete similarity cannot be achieved using two turbo-machines with different working fluids, even at the best efficiency point for particular expansion ratio. Constant $\Delta h_{0s}/a_{01}^2$ is imposed to achieve similarity, but the volumetric ratio is varying using different working fluids due to the variation of sound speed. The differences in the fluid properties and the expansion ratio lead to the deviation in turbine performance parameters, velocity diagram, turbine's exit swirl angle, and entropy generation. The use of $\Delta h_{0s}/a_{01}^2$ further limits the application of the gas turbine for refrigerants with heavier molecular weight to a pressure ratio less than the designed pressure ratio using air. The specific speed at the best efficiency point with different expansion ratio was shifted to a higher value if higher expansion ratio was imposed. A correction chart for R245fa was attempted to estimate the turbine's performance at higher expansion ratio as a function of volumetric ratio.

1. INTRODUCTION

The adaptation of an existing turbines for ORC application using different working medium can reduce the developmental effort involved in turbomachinery design aspects, such as re-designing the turbine wheel, prototyping and re-conducting the laboratory testing. The lack of documentation in literature about the adaptation of off-the-shelf turbines in applications other than the application for which they were originally designed has impeded the further development for ORC new-entrants. Turbines are usually designed for a particular set of specific speed and operating conditions, for a specific working fluid and a specific application. The adaptation of an existing turbine for the ORC application using a different working medium is fundamentally subjected to the similitude of the design analysis of turbomachinery, which is also known as similarity concept.

. Non-dimensional parameters of turbomachines for similarity concept have been derived using the Buckingham Pi theorem. In turbomachinery there are numerous dimensionless groups possible from the seven fundamental variables, such as flow coefficient, head coefficient, power coefficient, and Reynolds number. These non-dimensional groups serve as fundamental parameters for turbomachines handling compressible or incompressible fluids. A number of other important turbine parameters include specific speed, specific diameter, and loading coefficients. The introduction of specific speed allowed the rapid development in the experimental testing of hydraulic turbines in the 1900s (Meher-Homji, 2000) and facilitated the selection of turbomachines' types for different applications (Balje, 1981). The performance mapping using flow coefficient and loading coefficient has facilitated the preliminary design process for both axial flow turbines (Dixon & Hall, 2010) and radial inflow turbines (Chen & Baines, 1994). These parameters also allow turbomachinery designers to scale a turbine from one application to another application, with different wheel size, different inlet operating conditions, and different working mediums (Aungier, 2006; Japikse & Baines, 1995).

Scaling of turbomachines using the previously discussed non-dimensional parameters is feasible if the machine is geometrically similar, which implies that the number of blades, blades thickness, blade angle, machine size, radii and operating clearance are scaled proportionally (Japikse & Baines, 1995). Scaling from large sizes to small sizes imposes some difficulties, attributed to the surface finish, the manufacturing limit and the increased cost for increased geometrical tightness at small size. The Reynolds number imposes the next major constraint, in which a correction factor has to be applied. A number of correction charts are recommended to take into account of the Reynolds number effect in the laboratory testing of centrifugal compressors at different operating conditions (Casey, 1985; Strub et al., 1987). The geometrical scaling of turbomachinery from one size to another requires the tip speed to be constant to maintain similar effects from windage loss, tip clearance loss, external losses and mechanical effects (Japikse & Baines, 1995).

Scaling of turbomachines for different operating conditions within the same working fluid is a common practice in turbomachinery testing. The inlet operating condition is scaled to reduce the pressure and temperature into the compressor or the turbine during the performance test. This practice can reduce the operational cost and the capital cost of the testing equipment. The Reynolds number cannot be scaled and a correction factor is required either from the published literature or based on in-house knowledge.

The increasing interest in Organic Rankine Cycles has prompted the need for ORC turbines that can operate with various working mediums. The most common working fluid in existing commercial installations is n-Pentane (working fluid patented by ORMAT) (S. Quoilin & Lemort, 2009). Other working fluids are actively proposed and recommended under different conditions for a better thermodynamic cycle efficiency (Bao & Zhao, 2013) and a more cost-efficient design of heat exchanger (Sylvain Quoilin, Declaye, Tchanche, & Lemort, 2011). The testing of the turbine, however, is not a simple task. A full scale ORC set-up is favorable for turbine performance test but it imposes high design, development, and installation cost and efforts in the concerns of system layout, pump, heat exchanger and piping. Refrigerants typically introduce some side effects to either the environment, atmosphere, and health and safety issues. The refrigerants have to be sealed properly with minimal leakage, which further increases the operational cost of the test facility. A simple compressed air test bench is favorable as the compressed air is safe to be released to the atmosphere without any environmental issues. The testing via compressed air, however, might introduce some important deviations, as the real gas effects cannot be accounted accurately. The variation of density of real gas across blade passage during the expansion process and the machine Reynolds number cannot be scaled precisely from one fluid to another, which further limits the similitude using real gas. The lack of published correction chart for Mach number and Reynolds number for different working mediums has further limited the application of the similarity concept. These issues make it difficult for the turbomachinery designers or the engineers to apply the turbine performance curve generated using compressed air to an application using real gas, such as n-Pentane.

This study explores the feasibility of utilizing the similarity concept to estimate the turbine performance using real gas. Three different approaches using the similarity concept were proposed to scale air performance data to generate performance curves for two refrigerants, namely R134a and R245fa. A full computational fluid dynamic (CFD) analysis was then performed to generate the performances curves for the selected refrigerants. The approaches using the similarity concept were then compared to the result from the CFD analysis. The most feasible approach in scaling a turbine from air to refrigerants was selected. The accuracy of the performance prediction through the similarity analysis of the ORC turbomachine was estimated. The deviation in turbine's performance for different working fluids was presented and discussed.

2. METHODOLOGY

An industrial gas turbine with published turbine geometry (Sauret, 2012) was selected for this study. The selected gas turbine was initially designed for Sundstrand Power Systems (SPS) T-100 Multipurpose Small Power Unit (MPSPU) with a single-shaft configuration to accommodate the ground-based auxiliary power application (Jones, 1996). The nominal power of the selected turbine is 37 kW with a growth capability up to 75 kW (Jones, 1996). A CFD model was previously conducted on the gas turbine using air as the working medium and the result from the numerical modelling was compared to the experimental data (Jones, 1996; Wong & Krumdieck, 2014). The result from the CFD model agreed with the experimental data with less than 1% error in term of total-to-static efficiency. The CFD method was employed to generate the performance curve using two selected refrigerants, namely R134a and R245fa to validate the precision and accuracy of three different approaches of similarity concept in scaling the gas turbine from one working medium with ideal gas behavior to another working medium with real gas behavior.

The first part of this study re-generated the performance map of the selected gas turbine using air as the working medium and the performance curve served as a benchmark to determine the turbine performance using R134a and R245fa via similarity concept. The fluid properties of air were estimated using polytropic ideal gas equations. Three different approaches for similarity analysis were applied in this study. The performance curve scaled from the air data was plotted as a function of velocity ratio and specific speed for comparison.

The second part utilized the CFD methodology as outlined in previous study (Wong & Krumdieck, 2014) to generate the performance map of the selected gas turbine using R134a and R245fa. The performance map generated from the CFD tools was compared to the scaled performance map. The fluid properties of the refrigerants were extracted from REFPROP developed by National Institute of Standards and Technology (E. W. Lemmon, Huber, M.L., McLinden, M.O, 2013), and the details of the mathematical expressions to represent the real gas behavior of the selected refrigerants should be referred to the work by Lemmon (E. W. Lemmon & Span, 2006). The three different approaches were compared to the performance map by CFD tools, and the accuracy of each method was discussed.

The third part discusses the deviation in the turbine's performance using different working fluids at the best efficiency point. The fluid flow field and the blade loading across the blade passage, the velocity diagram at the turbine inlet and the outlet, and the Reynolds number effect on the turbine's performance were investigated. The limitation of the selected approach was presented, and a correction factor was generated to predict the best efficiency point of the turbine at higher expansion ratio (including super-sonic expansion).

2.1 Similarity Analysis

Similarity analysis, or similitude, provides a quick solution to scale a fluid machine for different operating conditions and different incompressible fluids without resorting to the full scale three-dimensional CFD methods. The performance of a turbomachine is dependent on the machine size, machine speed, and the fluid properties. Turbomachines are designed to handle either compressible or incompressible flow. Two extra terms are employed for turbomachines handling compressible flow, compared to the fluid machines handling incompressible flow, to take account of the compressible flow properties and the change of density during the expansion/compression process (Dixon & Hall, 2010). The performance parameters of a compressible flow turbomachine is expressed as a function of some variables, as listed in equation (1).

$$\Delta h_{0s}, P, \eta = f(N, D, \dot{m}, \rho_{01}, a_{01}, \gamma, \mu) \tag{1}$$

Where Δh_{0s} is the total-to-static enthalpy drop of the fluid across the turbine at the designed pressure ratio, P is the shaft power, η is the isentropic efficiency, and the efficiency is evaluated using the inlet stagnation and outlet static condition in this study, N is the rotational speed of the shaft, D is the diameter of the turbine wheel, $\dot{m}$ is the inlet mass flow rate, ρ_{01} is the density evaluated using the inlet stagnation condition, a_{01} is the sonic velocity at the inlet, γ is the specific heat, and μ is the dynamic viscosity. Buckingham π theorem was applied in equation (1) and three variables, density, ρ_{01}, shaft speed, N, and wheel diameter, D were selected to reduce the original expression into five dimensionless groups, as presented in equation (2). The full mathematical derivation should be referred to the work by Dixon (Dixon & Hall, 2010).

$$\frac{\Delta h_{0s}}{a_{01}^2}, \eta, \frac{P}{\rho_{01} a_{01}^3 D^5} = f\left\{\frac{\dot{m}}{\rho_{01} N D^3}, \frac{\rho_{01} N D^2}{\mu}, \frac{ND}{a_{01}}, \gamma\right\} \tag{2}$$

The current dimensionless group is not an explicit formulation where the parameters, such as density and sonic velocity, cannot be measured directly. The dimensionless groups can be reduced to a number of variables which allows direct measurement from the experiments if the compressible flow is modelled as a perfect gas. The dimensionless parameters were then reduced to a function of temperature and pressure at both inlet and outlet stations of the turbine, as listed in equation (3).

$$\frac{p_{02}}{p_{01}}, \eta, \frac{\Delta T_0}{T_{01}} = f\left\{\frac{\dot{m}\sqrt{\gamma R T_{01}}}{p_{01} D^2}, \mathrm{Re}, \frac{ND}{\sqrt{\gamma R T_{01}}}, \gamma\right\} \tag{3}$$

Where p is pressure, T is temperature, Re is machine Reynolds number, and R is the gas constant. The mathematical simplification of the dimensionless groups using perfect gas model are available from the works by Baines, Aungier, and Dixon (Aungier, 2006; Dixon & Hall, 2010; Japikse & Baines, 1995). Complete similarity can be achieved when

1) complete geometrical similarity is achieved (Aungier, 2006; Japikse & Baines, 1995), in which the turbine is scaled up or scaled down proportionally, *and*
2) dynamic similarity is achieved, in which the velocity components and forces are equal (Aungier, 2006).

Three different approaches are trialed to scale the performance data using air into the performance map using refrigerants. The scaled performance curve from each approach was compared to the performance curve from CFD analysis and the accuracy for each method was evaluated.

The *perfect gas approach* assumes that the selected refrigerants, R245fa and R134a are perfect gas. Three non-dimensional groups are hold constant, which are pressure ratio, blade speed coefficient in equation (4), and mass flow coefficients in equation (5). The outlet static pressure of the refrigerants is determined given the pressure ratio of the turbine using air. Equation (4) is employed to calculate the shaft's rotational speed whereas equation (5) is applied to determine the mass flow rate at the turbine inlet.

$$\frac{ND}{a_{01}} = \text{constant} \tag{4}$$

$$\frac{\dot{m}}{\rho_{01} N D^3} = \text{constant} \tag{5}$$

The <u>*variable pressure ratio approach*</u> is similar to the perfect gas approach, but the pressure ratio does not remain constant. The pressure ratio using the selected refrigerants is determined using the correlation in equation (6). Equation (4) and equation (5) are then employed to determine the shaft speed and the mass flow rate, respectively.

$$\frac{\Delta h_{0s}}{a_{01}^2} = \text{constant} \tag{6}$$

The <u>*constant specific speed approach*</u> assumes constant pressure ratio, velocity ratio, υ and the specific speed, N_s for the selected working medium. The optimal velocity ratio and specific speed of a turbomachine typically fall in a narrow range of operation for maximum efficiency. Both are hold constant to determine the shaft speed and the mass flow rate by using equations (7) and (8), respectively.

$$\nu = \frac{U}{C_{is}} = \frac{U}{\sqrt{2\Delta h_{0s}}} \tag{7}$$

Where U is turbine inlet tip speed, and C_{is} is the fictitious velocity when the fluid is expanded in an isentropic process across a nozzle, with the pressure ratio equals to the pressure ratio of the turbine stage.

$$N_s = \frac{\omega\sqrt{\dot{m}/\rho_{exit}}}{\Delta h_{0s}{}^{0.75}} \tag{8}$$

Where ρ_{exit} is the density at the turbine outlet.

2.2 Evaluation of Aerodynamic Performance using CFD Analysis

CFD analysis was conducted on the gas turbine to determine the overall performance of the turbine stage and evaluate the fluid dynamics across the blade passage. The CFD analysis was performed using ANSYS CFX version 15.0 and the overall procedure is illustrated in Figure 1. The solid models of both nozzle and rotor blades were constructed in ANSYS BladeGen by providing the principal geometry and the distribution of the wrap angle along the meridional position. Hexahedral meshes were then applied on the fluid zone across both the nozzle and turbine blades. A two-dimensional topography was generated on the hub surface, mid span and close-to-shroud surface as a framework to smoothen the formation of meshes. The mesh quality was controlled by refining the mesh size and manipulating the number of elements across the boundary layer of the blade surface. The skew meshes were eliminated to avoid ill-meshes. The operating condition and the boundary condition were then set up at each stations (nozzle inlet, interface between nozzle and turbine rotor, and rotor outlet). A suitable working fluid was selected from the in-built fluid database or the fluid properties can also be imported from the external fluid database. *k*-*ε* model was selected to model the turbulence across the blade passage. The

Navier-Stokes equations were solved numerically and the result was evaluated as velocity vector field and distribution of thermodynamics properties across the blade passage.

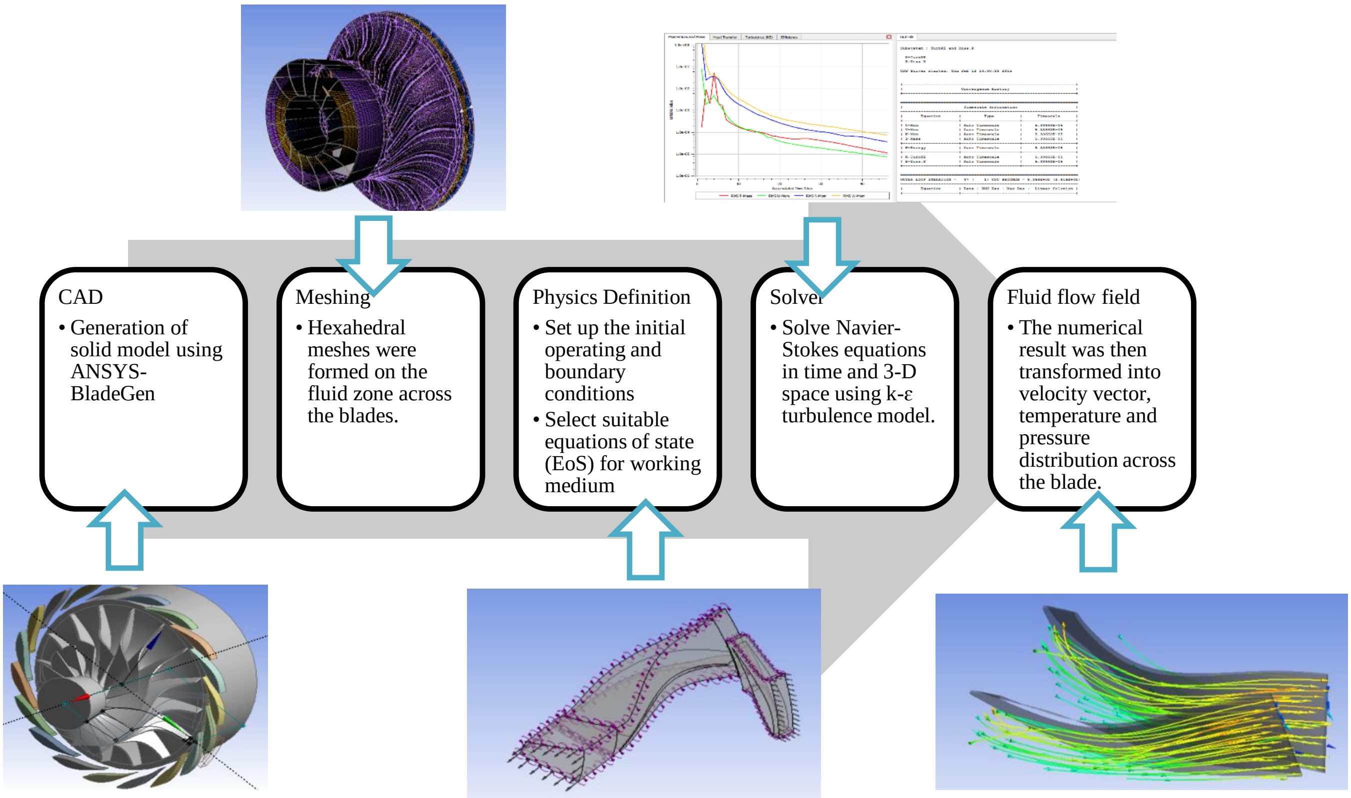

Figure 1: Overall procedures of CFD simulation using ANSYS Turbomachinery Package

3. RESULT

The three different approaches were applied to scale the performance curve from air to R134a and R245fa with the operating conditions in Table 1.

Table 1: Operating condition of air and selected refrigerants

	Unit	Air	R134a	R245fa
Molecular weight, M	g/mol	28.97	102.03	134.05
Inlet total temperature	K	1056.5	386	406.1
Inlet total pressure	kPa	580.4	2380	2334
Compressibility factor at inlet	-	1	0.786	0.630
Speed of sound at inlet	m/s	635	153.4	108.6
Outlet static pressure	kPa	101.3	420	420
Compressibility factor at outlet	-	1	0.931	0.904

R134a was superheated up to 35 degree before entering the turbine to avoid the formation of moisture at the end of the expansion process since it is a wet fluid. The scaled performance curves of R134a using the three approaches were compared to the result from the CFD analyses, in terms of velocity ratio in Figure 2, and specific speed in Figure 3. The three similarity approaches and the CFD analyses were compared in term of specific speed for R134a in Figure 3, and R245fa in Figure 4.

The *perfect gas approach* shows that the optimal velocity ratio is under-estimated. The optimal value from the *perfect gas approach* is 0.48, whereas the estimated value from the CFD analysis is 0.60.

The optimal velocity ratio from the *variable pressure ratio approach* and the *constant specific speed approach* agrees closely to the estimated values from the CFD analysis, with an error less than 10%, as illustrated in Table 1. The optimal operating shaft speed would be predicted incorrectly if the *perfect gas approach* was applied.

The overall trend of the turbine performance is similar between the CFD analysis and the *constant specific speed* approach, but the trend is different for the *variable pressure ratio* approach. The *variable pressure ratio* approach shows fairly flat efficiency for the range of velocity ratio between 0.55 and 0.70, and the range of specific speed between 0.33 and 0.42. However, the CFD analysis shows that the turbine is very sensitive to the operating point, as shown in Figure 2 and Figure 3. The turbine performance drops significantly at the operating points away from the best efficiency point. The best efficiency point is defined as the point with the maximum total-to-static isentropic efficiency at certain pressure ratio. The result shows that the *variable pressure ratio* approach provides a good prediction of optimal velocity ratio, optimal specific speed, and maximum efficiency. However, the approach does not provide a good estimation of performance for the operating points away from the best efficiency point, as presented in Table 2.

The *constant specific speed* approach assumes constant pressure ratio, specific speed and velocity ratio. The trend of the performance is similar between the *constant specific speed* approach and the CFD analysis for R134a and R245fa, based on Figure 3 and Figure 4. However, the turbine efficiency was over-estimated with errors between 10 and 20%, for the investigated range of velocity ratio and specific speed. This approach provides a better estimation in the turbine performance away from the best efficiency point, compared to another two approaches. However, the *constant specific speed* approach yields over 10% error in estimating the optimal velocity ratio, optimal specific speed, and maximum turbine efficiency, whereas the *variable pressure ratio* approach yields an error between 7% and 8%, as listed in Table 2.

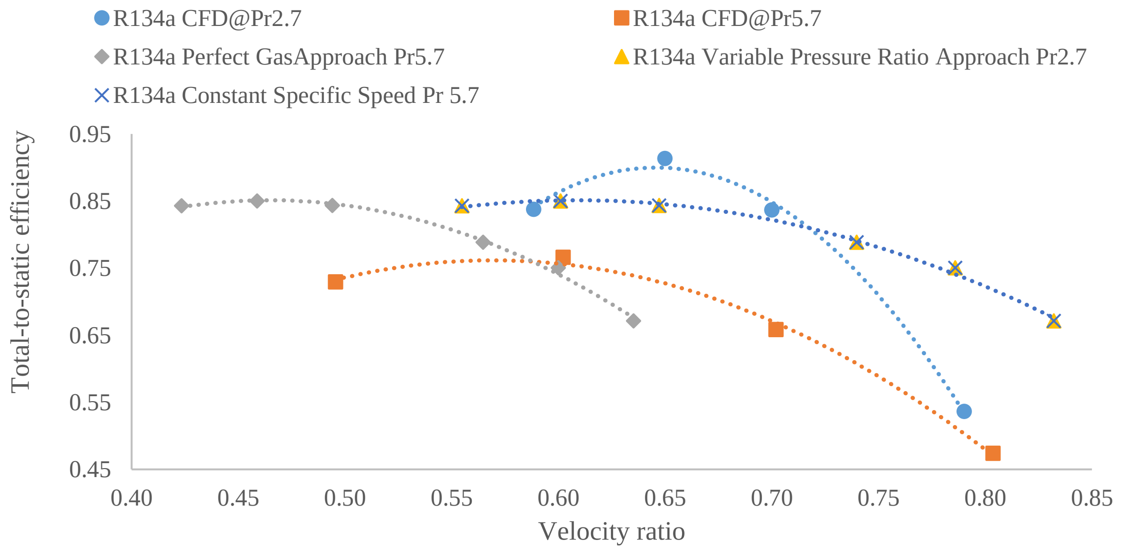

Figure 2: Comparisons of scaled performance from air data and CFD result for R134a as a function of velocity ratio

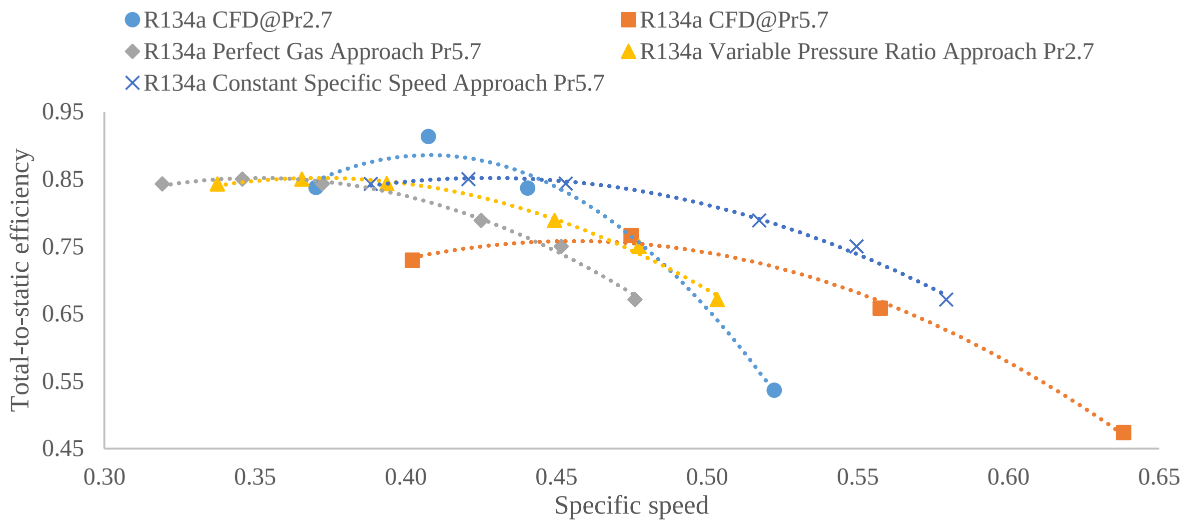

Figure 3: Comparisons of scaled performance from air data and CFD result for R134a as a function of specific speed

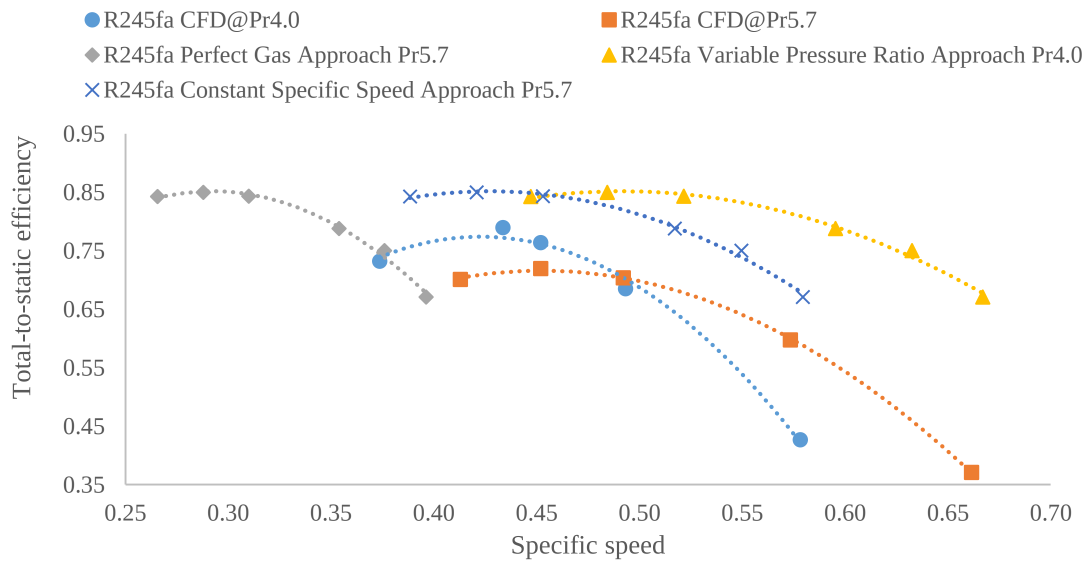

Figure 4: Comparisons of scaled performance from air data and CFD result for R245fa as a function of specific speed

The estimation of the inlet mass flow rate by the three similarity approaches and the CFD analysis was compared. The *perfect gas* approach and the *variable pressure ratio* approach utilize the mass flow coefficient in equation (5) whereas the *constant specific speed* approach uses the specific speed correlation in equation (8) to estimate the inlet mass flow rate. The result in Table 2 shows that the mass flow rate was under-estimated using all three approaches. The mass flow coefficient predicts the inlet mass flow rate with a better accuracy, with an error less than 10%, as opposed to the specific speed correlation, with error in the range of 15 and 25%. Hence, the *perfect gas* approach and the *variable pressure ratio* approach provide better estimations in the inlet mass flow, compared to the *constant specific speed* approach.

Table 2: Numerical error for different scaling approaches

	Working medium	Pressure ratio	Optimal velocity ratio	Optimal specific speed	Maximum total-to-static efficiency	Mass flow rate (kg/s)	Average Error (%)
Benchmark	Air	5.7	0.6	0.42	0.85	0.29	
Approach 1 (Perfect Gas)	R134a	5.7	0.46	0.35	0.85	3.46	
	Error (%)		23.3	25.5	11.8	4.6	16.3
	R245fa	5.7	0.38	0.29	0.85	3.75	
	Error (%)		31.9	35.9	18.4	9.0	23.8
Approach 2 (Variable Pressure Ratio)	R134a	2.7	0.6	0.37	0.85	3.46	
	Error (%)		7.7	9.8	6.6	4.7	7.2
	R245fa	4.0	0.6	0.48	0.85	3.75	
	Error (%)		2.9	13.5	9.4	9.0	8.7
Approach 3 (Constant Specific Speed)	R134a	5.7	0.6	0.42	0.85	2.99	
	Error (%)		0.0	10.6	11.8	17.6	10.0
	R245fa	5.7	0.6	0.42	0.85	3.15	
	Error (%)		7.5	7.2	18.4	23.5	14.1
CFD	R134a	2.7	0.65	0.41	0.91	3.63	
		5.7	0.60	0.47	0.76	3.63	
	R245fa	4.00	0.58	0.42	0.78	4.12	
		5.7	0.56	0.45	0.72	4.12	

4. DISCUSSION

The discrepancy in the turbine efficiency if a turbine stage is scaled from one operating condition into another is attributed to the variation in machine Reynolds number and Mach number. Various Reynolds number corrections were proposed for centrifugal compressors, such as ASME PTC-10 (PTC, 1997) and the efficiency-deficiency chart by Pampreen (Pampreen, 1973). The machine Reynolds number, however, does not have significant effect on the change in efficiency in this study as the effects of viscosity and thermal conductivity can be neglected at high Reynolds number (Harinck, Guardone, & Colonna, 2009). Reynolds number, $Re=\rho UD/\mu$ is a function of density, ρ, tip speed, U, wheel diameter, D, and dynamic viscosity, μ. The dynamic viscosity of the refrigerants is much smaller, rendering a higher value in the Reynolds number, in the magnitude of 100 x 10^6, as opposed to the Reynolds number of steam, air, and water in the magnitude of 1 x 10^6. The turbine inlet condition was varied using the CFD analysis to investigate the correlation between the machine Reynolds number and the turbine performance, as illustrated in Figure 5. The turbine's performance is fairly consistent in a wide range of Reynolds number, between 10 and 90. Hence, the Reynolds number effect can be neglected in this study.

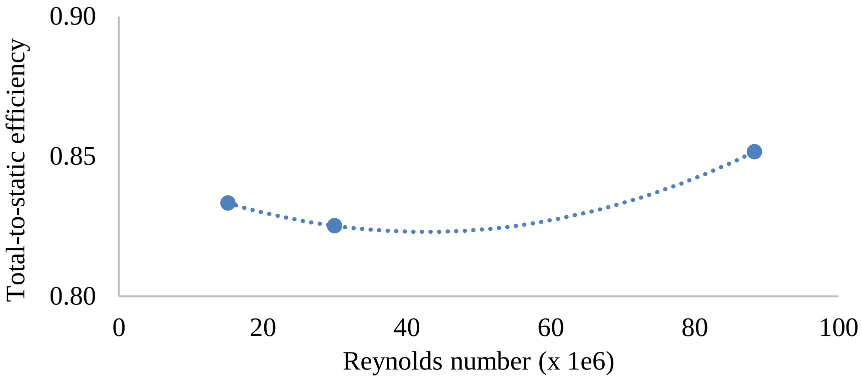

Figure 5: Effect of machine Reynolds number on turbine's performance using R134a

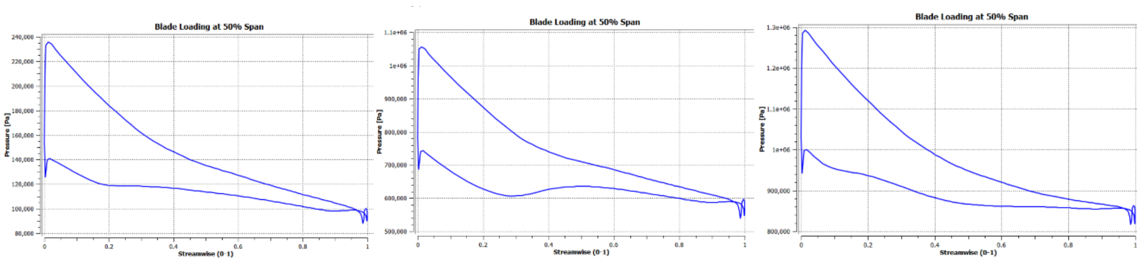

(a) (b) (c)

Figure 6: Blade loading and density at blade surface using air at pressure ratio of 5.7 (a), R245fa at pressure ratio of 4.0 (b) and R134a at pressure ratio of 2.7 (c)

The blade loading along the pressure and suction surfaces at optimal specific speed using the *variable pressure ratio* approach are similar for all three working fluids; air, R134a and R245fa. Constant pressure drop was observed for air (modelled as ideal gas), R134a and R245fa (modelled as real gas) along pressure surface, but pressure fluctuation was observed for R245fa along the suction surface. The fluctuation is related to the adverse pressure gradient near the leading edge of the suction surface, which forms a vortex and local backpressure downstream of the vortex, as illustrated by the velocity vector in Figure 7. The flow re-attaches downstream of the vortex with gradual pressure drop along the blade passage.

The maximum isentropic efficiency for air, R134a and R245fa is different although the pressure loading along the blade passage at the optimal specific speed is similar. The highest turbine efficiency is achieved by R134a, followed by air, and R245fa. The deviation can be explained as a function of compressibility effect. The compressibility factor is a ratio of actual specific volume to the ideal volume of selected fluids. The compressibility effect of the expansion process across the turbine was measured qualitatively by volumetric flow ratio (Macchi & Perdichizzi, 1981). Macchi and Perdichizzi found that the increase in the volumetric flow ratio gives rise to a reduction in the turbine efficiency at optimal specific speed (Macchi & Perdichizzi, 1981), and the volumetric flow ratio has to be less than 50 to achieve a high turbine stage efficiency greater than 0.80 (Angelino, Invernizzi, & Macchi, 1991). The volumetric flow ratio is different for different working fluid using the *variable pressure ratio* approach. The volumetric flow ratio was determined as 5.7 for air, 4.9 for R245fa, and 2.7 for R134a. The use of equation (9) justifies the highest efficiency using R134a at low pressure ratio. Equation (9) is the change of entropy of a perfect gas in a closed system.

$$\Delta s = c_v \ln\left({}^{T_3}\!/_{T_1} \right) + R \ln\left({}^{v_3}\!/_{v_1} \right) \tag{9}$$

Where *Δs* denotes the entropy generation, c_V isochoric heat capacity, *R* specific gas constant, *T* temperature, and *v* specific volume. The increase in volumetric flow ratio generates a larger entropy difference. The larger the entropy differences, the larger the irreversibility of the system and the lower the turbine's efficiency. Hence, the highest efficiency is achieved by R134a with the lowest pressure ratio among all three working fluids. However, the turbine's efficiency using R245fa (expansion ratio of 4.9) is 78%, which is lower than air at 85% (expansion ratio of 5.7). This shows that the volumetric flow ratio is not the sole contributor to the drop in turbine performance using different fluids.

Table 3: Performance parameters for different working fluids, using Variable Pressure Ratio Approach

Fluids	Air	R134a	R245fa
Velocity triangle	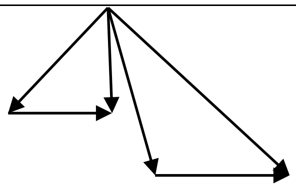	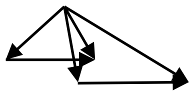	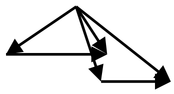
Pressure ratio	5.7	2.7	4.0
Volumetric flow ratio	5.7	2.7	4.9
Degree of Reaction	0.42	0.47	0.44
Flow coefficient	0.245	0.172	0.249
Stage loading coefficient	1.040	0.974	0.995

The differences in the volumetric flow ratio also gives rise to the change in a number of turbine parameters. Optimum degree of reaction decreases whereas optimal flow coefficient increases with increasing expansion ratio. These yield some changes in the velocity diagram at the turbine exit, as shown in Table 3. The complete similarity is not achieved as the velocity vector at the turbine exit is not conserved. Hence, the *variable pressure ratio* approach does not achieve complete similarity, and this gives rise to the error in estimating the velocity ratio, specific speed, and turbine performance.

The flow field diagrams of R245fa, R134a, and air using the *variable pressure ratio* approach were compared in Figure 7. The flow undergoes turning from axial direction to tangential direction, and gives rise to Coriolis effect in the radial direction (Moustapha, Zelesky, Baines, & Japiske, 2003). The flow undergoes a non-uniform velocity distribution in the spanwise direction, with lowest velocity near the end wall surface of the hub. The radial gradient of the flow velocity in the spanwise direction gives rise to the imbalance in the pressure gradient in the spanwise direction. The end result of the Coriolis effect and the non-uniform velocity give rise to a complex flow field, which is illustrated in Figure 7 in term of flow angle. The bulk flow moves from suction surface near the shroud to pressure surface near the hub. The flow is compensated by a number of passage vortices, and the flow vector diagram can be found in Kitton's work (also presented by Baines in his work (Moustapha et al., 2003)). This phenomena exists in the best efficiency point, attributed to the turning of the flow from axial to tangential direction. The distribution of the swirl angle at the trailing edge was averaged and the flow angle was determined as 1˚ for air, 33° for R134a and 37° for R245fa. The result implies that the turbine exit swirl angle might increase monotonically with the molecular weight of the working fluids, with the highest by R245fa and the lowest by air. Positive swirl angle is non-favorable as the fluid internal energy would be lost as kinetic energy. The specific work output would decrease with a positive swirl angle, based on Euler turbomachinery equation.

$$W_x = U_2 C_{\theta 2} - U_3 C_{\theta 3} = U_2 C_{m2} \tan\alpha_2 - U_3 C_{m3} \tan\alpha_3 \tag{10}$$

Where W_X is specific work output, U_2 is rotor inlet tip speed, U_3 is rotor outlet tip speed, C_θ is tangential velocity component, C_m is meridional velocity component, and *α* is swirl angle.

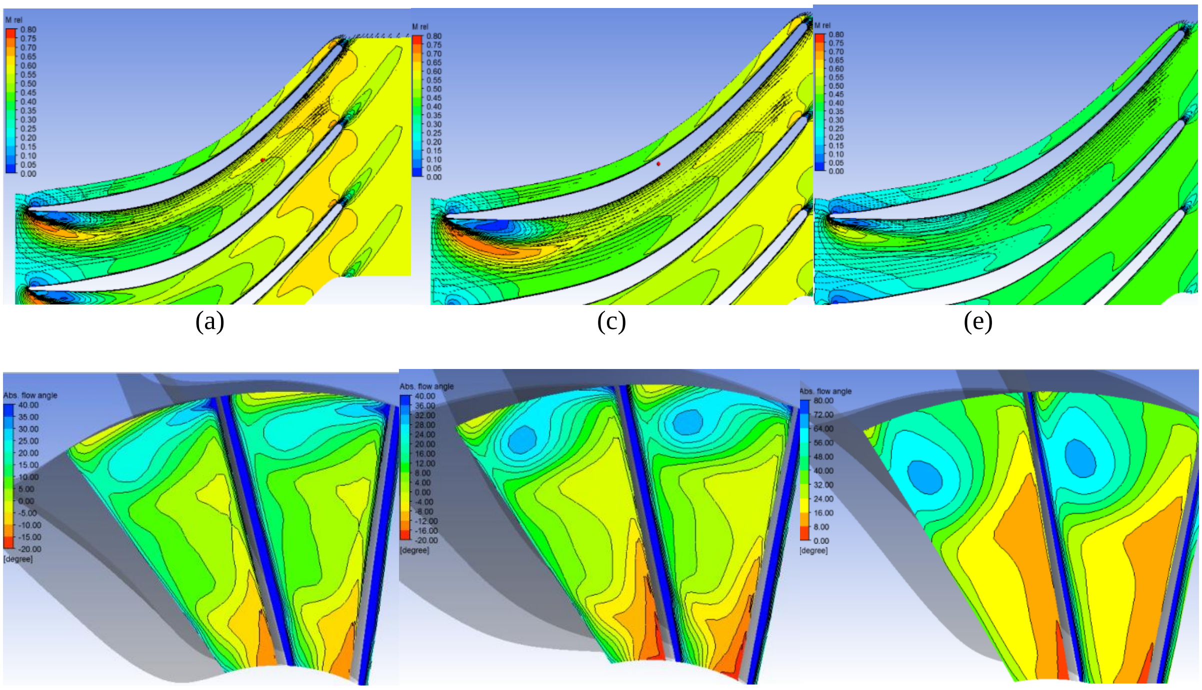

(a) (c) (e)

(b) (d) (f)

Figure 7: Distribution of relative Mach number in the meridional plane and distribution of absolute flow angle at the trailing edge using air at pressure ratio of 5.7 (a-b), R245fa at pressure ratio of 4.0 (c-d) and R134a at pressure ratio of 2.7 (e-f)

The conventional radial inflow turbine is typically designed for low pressure ratio application, which is between 1.2 and 3.0 for automotive turbochargers, and less than 10 for single stage gas turbines to avoid choking and shock waves in supersonic expansion. The selected gas turbine has a design pressure ratio of 5.7. Different pressure ratio was determined for R134a and R245fa assuming constant value of $\Delta h_{0s}/a_{01}^2$ (using the *variable pressure ratio* approach) and plotted in Figure 8. The limiting line on the left represents the saturation lines of the refrigerants. The calculated pressure ratio for the selected refrigerants is less than 5.7, which is the pressure ratio imposed on the turbine using air. The local sound speed of refrigerants with heavier molecular weight is less than the local speed of sound using air. The local speed of sound is between 90 and 190 m/s for R134a and between 75 and 160 m/s for R245fa for the temperature range of 300 and 450 K, and pressure range of 0.5 and 4.0 MPa, which is less than the local speed of sound of air at 635 m/s with the given operating condition in Table 1. The smaller the local speed of sound, the smaller the isentropic enthalpy drop and the smaller the pressure ratio across the turbine. Hence, the *variable pressure ratio* approach is limited to a pressure ratio less than the design pressure ratio using air. This limits the applicability of the approach in ORC application, which is characterized for high pressure ratio expansion.

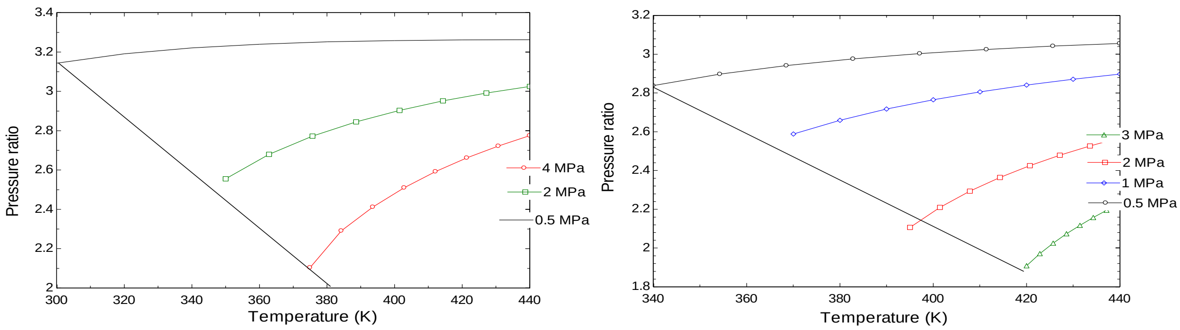

(a) (b)

Figure 8: Range of applicability using equation (6) for R134a (a) and R245fa (b)

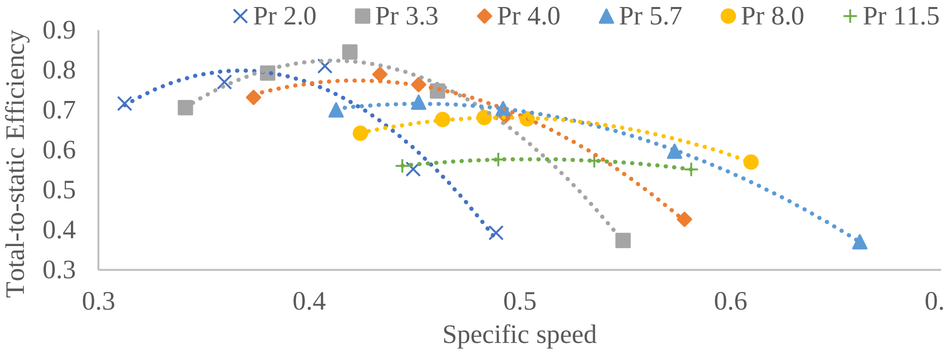

Figure 9: Performance map of R245fa at different specific speed and pressure ratio

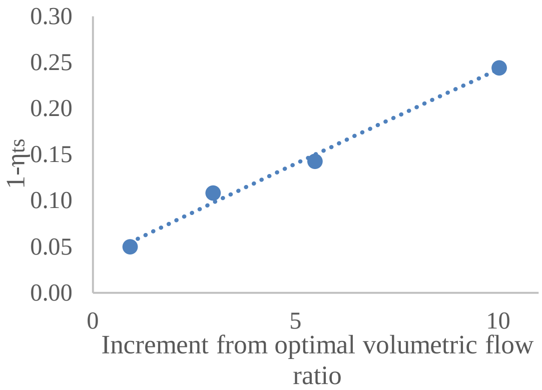

(a)

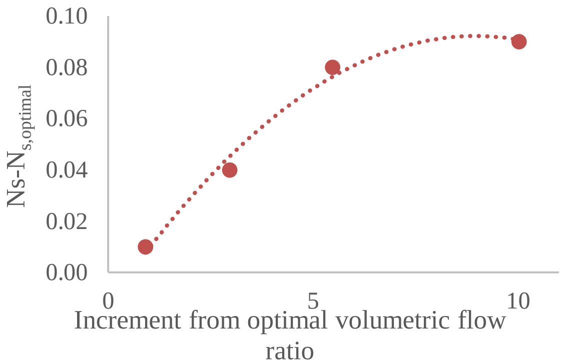

(b)

Figure 10: Deviation of best efficiency point and the corresponding specific speed at increasing volumetric flow ratio

The prediction of the turbine performance at higher pressure ratio or expansion ratio is required for ORC application. A correction chart for R245fa at different expansion ratio was developed using Figure 9. The turbine's performance map for R245fa was generated for different pressure ratio (2 – 11.5) and specific speed (0.3 – 0.7), and plotted in Figure 9. The result shows that the maximum turbine performance was achieved at a pressure ratio of 3.3 (equivalent to volumetric flow ratio at 4.0). The maximum efficiency point at the pressure ratio of 3.3 iss used as a benchmark to calculate the deficiency in efficiency and deviation of optimal specific speed at higher volumetric flow ratio. The turbine losses increases linearly with increasing volumetric flow ratio as shown in Figure 10(a). The location of the specific speed for the best efficiency point at increasing volumetric ratio is increasing, as shown in Figure 9. The deviation in the optimal specific speed is plotted as a function of volumetric flow ratio in Figure 10. The result shows that the deviation in optimal specific speed increases with increasing volumetric flow ratio until the blade passage is choked (with the relative Mach number around 1). The further increment in volumetric flow ratio does not have any effect on the value of N_s-$N_{s,optimal}$, as illustrated in Figure 10.

5. CONCLUSION

Three different approaches using the similarity concept were proposed and investigated to scale the selected gas turbine from air to R134a and R245fa in this study. The *perfect gas* approach assuming the real gas as perfect gas provides the largest error in terms of optimal velocity ratio, optimal specific speed, and maximum efficiency. The *variable pressure ratio* approach shows the highest averaged accuracy in predicting the optimal velocity ratio, optimal specific speed, maximum efficiency and mass flow rate. The *constant specific speed* approach is recommended to estimate the turbine's performance away from the best efficiency point.

Constant value of $\Delta h_{0s}/a_{01}^2$ was imposed in the *variable pressure ratio* approach to achieve the similarity but a number of deviations was observed, including swirl angle at the turbine outlet, volumetric flow ratio, best efficiency point and the corresponding specific speed. The Reynolds number effect does not influence the scaling using refrigerants as the effect of viscosity is negligible at high Reynolds number using refrigerants with low viscosity. The swirl angle at the turbine outlet was observed as a function of molecular weight, in which the increment in molecular weight increases the swirl angle and reduces the specific work output. The *variable pressure ratio* approach does not ensure a constant volumetric flow ratio, hence the complete similarity cannot be achieved. The *variable pressure ratio* approach is limited to pressure ratio less than the design pressure ratio using air, which is not suitable to scale an ORC turbine. Therefore, a correction chart was developed to scale the performance of the gas turbine for higher volumetric ratio using R245fa. The deficiency in turbine efficiency is linearly correlated to the increased volumetric flow ratio. The correction chart provides a good estimation in selecting a suitable turbine for a particular ORC application. However, the correction chart has to be validated against the experimental data for better accuracy.

NOMENCLATURE

a	local speed of sound	(m/s)
C	absolute flow velocity	(m/s)
C_{is}	isentropic flow velocity	(m/s)
c_v	isochoric heat capacity	(J/kg.K)
D	turbine wheel diameter	(m)
Δh_0	enthalpy drop	(kJ/kg)
$\dot{m}$	mass flow rate	(kg/s)
N	shaft speed	(rev/min)
N_s	specific speed	(-)
p	pressure	(kPa)
P	shaft power	(kW)
R	gas constant	(J/kg.K)
Re	Reynolds number	(-)
T	temperature	(K)
U	tip speed	(m/s)

Greek letter

α	swirl angle	(degree)
θ	tangential direction	(-)
γ	ratio of specific heats	(-)
η	efficiency	(-)
ρ	density	(kg/m^3)
υ	velocity ratio	(-)
ω	shaft speed	(rad/s)

Subscript

01	nozzle inlet stagnation condition
02	rotor inlet stagnation condition
03	rotor outlet stagnation condition
1	nozzle inlet static condition
2	rotor inlet static condition
3	rotor outlet static condition
m	meridional plane
s	isentropic process

REFERENCES

Angelino, G., Invernizzi, C., & Macchi, E. (1991). Organic Working Fluid Optimization for Space Power Cycles. In G. Angelino, L. De Luca & W. A. Sirignano (Eds.), *Modern Research Topics in Aerospace Propulsion* (pp. 297-326): Springer New York.

Aungier, R. H. (2006). *Turbine aerodynamics: axial-flow and radial-inflow turbine design and analysis*: ASME Press.

Balje, O. E. (1981). *Turbomachines: A Guide to Design Selection and Theory*: Wiley.

Bao, J., & Zhao, L. (2013). A review of working fluid and expander selections for organic Rankine cycle. *Renewable and Sustainable Energy Reviews, 24*, 325-342.

Casey, M. V. (1985). The Effects of Reynolds Number on the Efficiency of Centrifugal Compressor Stages. *Journal of Engineering for Gas Turbines and Power, 107*(2), 541-548. doi: 10.1115/1.3239767

Chen, H., & Baines, N. C. (1994). The aerodynamic loading of radial and mixed-flow turbines. *International Journal of Mechanical Sciences, 36*(1), 63-79. doi: 10.1016/0020-7403(94)90007-8

Dixon, S. L., & Hall, C. (2010). Fluid Mechanics and Thermodynamics of Turbomachinery Retrieved from http://canterbury.eblib.com.au/patron/FullRecord.aspx?p=534952

Harinck, J., Guardone, A., & Colonna, P. (2009). The influence of molecular complexity on expanding flows of ideal and dense gases. *Physics of Fluids (1994-present), 21*(8), 086101. doi: doi:http://dx.doi.org/10.1063/1.3194308

Japikse, D., & Baines, N. C. (1995). *Introduction to turbomachinery*: Concepts ETI.

Jones, A. C. (1996). Design and Test of a Small, High Pressure Ratio Radial Turbine. *Journal of Turbomachinery, 118*(2), 362-370. doi: 10.1115/1.2836651

Lemmon, E. W., Huber, M.L., McLinden, M.O. (2013). NIST Standard Reference Database 23: Reference Fluid Thermodynamic and Transport Properties-REFPROP, Version 9.1. Gaithersburg: Standard Reference Data Program.

Lemmon, E. W., & Span, R. (2006). Short fundamental equations of state for 20 industrial fluids. *Journal of Chemical & Engineering Data, 51*(3), 785-850.

Macchi, E., & Perdichizzi, A. (1981). Efficiency prediction for axial-flow turbines operating with nonconventional fluids. *ASME Journal of Engineering for Power, 103*, 718e724.

Meher-Homji, C. B. (2000). *'The Historical Evolution of Turbomachinery.* Paper presented at the Proceedings of the 29th Turbomachinery Symposium, Texas A&M University, Houston, TX.

Moustapha, H., Zelesky, M., Baines, N. C., & Japiske, D. (2003). *Axial and Radial Turbines*: Concepts Eti.

Pampreen, R. (1973). Small turbomachinery compressor and fan aerodynamics. *Journal of Engineering for Gas Turbines and Power, 95*(3), 251-256.

PTC, A. (1997). PTC 10-1997, Performance test code on compressors and exhausters. *American Society of Mechanical Engineers, New York, 3*.

Quoilin, S., Declaye, S., Tchanche, B. F., & Lemort, V. (2011). Thermo-economic optimization of waste heat recovery Organic Rankine Cycles. *Applied Thermal Engineering, 31*(14–15), 2885-2893. doi: 10.1016/j.applthermaleng.2011.05.014

Quoilin, S., & Lemort, V. (2009, 14-17 April). *Technological and economical survey of Organic Rankine Cycle systems.* Paper presented at the 5th European Conference Economis and Management of Energy in Industry, Algarve, Portugal.

Sauret, E. (2012). *Open design of high pressure ratio radial-inflow turbine for academic validation.* Paper presented at the Proceedings of the ASME 2012 International Mechanical Engineering Congress and Exposition, Houston, Texas.

Strub, R. A., Bonciani, L., Borer, C. J., Casey, M. V., Cole, S. L., Cook, B. B., . . . Strite, M. A. (1987). Influence of the Reynolds Number on the Performance of Centrifugal Compressors. *Journal of Turbomachinery, 109*(4), 541-544. doi: 10.1115/1.3262145

Wong, C. S., & Krumdieck, S. (2014). *Energy and Exergy Analysis of an Air-Cooled Geothermal Power Plant with Fixed Nozzle Turbine in Subsonic Expansion and Supersonic Expansion via CFD Analysis.* Paper presented at the 36th New Zealand Geothermal Workshop Auckland University.

ACKNOWLEDGEMENT

The project is supported by Heavy Engineering Research Association (HERA) as part of the Above Ground Geothermal and Allied Technology (AGGAT) program with funding from NZ Ministry for Business, Innovation and Employment contract: HERX1201.